View metadata, citation and similar papers at core.ac.uk
brought to you by CORE
provided by Repositori d'Objectes Digitals per a l'Ensenyament la Recerca i la Cultura

DSF-24/2006, IFIC/06-21, MPP-2006-89

Ultra High Energy Neutrinos in the Mediterranean: detecting ν_τ and ν_μ with a km^3 Telescope

A. Cuoco[1], G. Mangano[1], G. Miele[1], S. Pastor[2], L. Perrone[3], O. Pisanti[1], and P.D. Serpico[4]

[1] Dipartimento di Scienze Fisiche, Università di Napoli *Federico II* and INFN Sezione di Napoli, Complesso Universitario di Monte S. Angelo, Via Cinthia, I-80126 Napoli, Italy.
[2] Instituto de Física Corpuscular (CSIC-Universitat de València), Ed. Institutos de Investigación, Apdo. 22085, E-46071 València, Spain.
[3] Dipartimento di Ingegneria dell'Innovazione, Università di Lecce and INFN Sezione di Lecce, Via per Monteroni, I-73100 Lecce, Italy.
[4] Max-Planck-Institut für Physik (Werner-Heisenberg-Institut), Föhringer Ring 6, D-80805 Munich, Germany.

Abstract. We perform a study of the ultra high energy neutrino detection performances of a km^3 Neutrino Telescope sitting at the three proposed sites for ANTARES, NEMO and NESTOR in the Mediterranean sea. We focus on the effect of the underwater surface profile on the total amount of yearly expected τ and μ crossing the fiducial volume in the limit of full detection efficiency and energy resolution. We also emphasize the possible enhancement of matter effect by a suitable choice of the geometry of the Telescope.

PACS numbers: 95.85.Ry, 95.55.Vj, 13.15.+g

arXiv:astro-ph/0609241v4 24 Feb 2007

1. Introduction

Neutrinos are one of the main components of the cosmic radiation in the ultra-high energy (UHE) regime. Although their fluxes are uncertain and depend on the production mechanism, their detection can provide information on the sources and origin of the UHE cosmic rays. For example, UHE neutrinos can be produced via π-photoproduction by strongly accelerated hadrons in presence of a background electromagnetic field. This scenario is expected to occur in extreme astrophysical environments like the jets of active galactic nuclei, radio galaxies and gamma ray burst sources as well as in the propagation of UHE nucleons scattering off the cosmic background radiation (known as *cosmogenic neutrinos* [1, 2]).

From the experimental point of view, after the first pioneering and successful achievements, neutrino astronomy in the high energy regime [3, 4, 5, 6, 7] is a rapidly developing field, with a new generation of neutrino telescopes on the way. A benchmark result was obtained by the DUMAND [8] collaboration, followed by the successful deployments of NT-200 at Lake Baikal [9] and AMANDA [10] at the South Pole, which have shown the feasibility of large optical Cherenkov neutrino telescopes (NT) in open media like sea- or lake-water and glacial ice. These experiments observed atmospheric neutrinos [11] and set bounds on their extraterrestrial flux [12, 13, 14] which are much more constraining than the corresponding bounds obtained by underground neutrino detectors [15]. These interesting results and the perspective to perform astronomical studies using UHE neutrinos stimulated several proposals and R&D projects for neutrino telescopes in the deep water of the Mediterranean sea, namely ANTARES [16], NESTOR [17, 18, 19] and NEMO [20], which in the future could lead to the construction of a km^3 telescope as pursued by the KM3NeT project [21, 22]. Actually, the ANTARES collaboration is in a more advanced phase, with a telescope with an area of ~ 0.1 km^2 already under construction [23]. A further project is IceCube, a cubic-kilometer under-ice neutrino detector [24, 25, 26] currently being deployed in a location near the geographic South Pole in Antarctica. IceCube applies and improves the successful technique of AMANDA to a larger volume.

Until now, the possibility to perform astronomy with neutrinos has been seriously limited by the presence of the heavy atmospheric background in the energy range presently explored. The start of ν-astronomy is eagerly waiting the completion of the new km^3 projects. In fact, according to theoretical expectations, the km^3 is the minimum detector size required to detect with reasonable chances of success point-like sources at the TeV scale and, more relevant for this paper, to explore energies above about 100 TeV, where extraterrestrial diffuse fluxes should start to dominate over the steeper atmospheric spectrum. In the following we shall focus the attention mainly on this energy range, although many of our results are valid also at lower energies.

Although NT's were originally thought as ν_μ detectors, their capability as ν_τ detectors has become a hot topic [27, 28, 29, 30, 31, 32, 33, 34, 35], in view of the fact that neutrino oscillations lead to nearly equal astrophysical fluxes for the three neutrino

flavors‡. Despite the different behavior of the produced tau leptons with respect to muons in terms of energy loss and decay length, both ν_μ and ν_τ detection are sensitive to the matter distribution near the NT site. Thus, a computation of the event detection rate of a km^3 telescope requires a careful analysis of the surroundings of the proposed site. The importance of the elevation profile of the Earth surface around the detector was already found of some relevance in Ref. [41], where some of the present authors calculated the aperture of the Pierre Auger Observatory [42, 43] for Earth-skimming UHE ν_τ's. Indeed, air shower experiments can be used as NT's at energies $\gtrsim 10^{18}$ eV, a topic recently reviewed in [44]. In particular, the possibility of detection of the τ leptons produced by Earth-skimming UHE ν_τ's has been analyzed in a series of papers [41], [45]-[55]. In Ref. [41] the use of a Digital Elevation Map (DEM) of the geographical area of the experiment proved useful to characterize peculiar matter effects in Earth-skimming events.

The aim of this paper is to estimate the effective aperture for ν_τ and ν_μ detection of a km^3 NT in the Mediterranean sea placed at any of the three locations proposed by the `ANTARES`, `NEMO` and `NESTOR` collaborations. We do not consider any detail related to the experimental setup nor the detector response. In particular, we assume full detection efficiency via Cherenkov radiation for muons and taus crossing the NT fiducial volume. This means that we consider a lepton as detected if it crosses in any point the surface delimiting our fiducial volume, without e.g. taking into account further requirements or cuts needed for a good directional or energy reconstruction. These would depend on several parameters, like the spacing of the strings, the distribution of photomultipliers along the string, etc. which are characteristics of the apparatus and thus beyond the aim of the present analysis. We rather compare the site characteristics by using the DEM of the different areas. We shall therefore characterize and quantify the importance of "matter effects" for the three sites, and focus on the role played by the geometry of the experiment in enhancing the effect. These considerations may provide an important ingredient in shaping the final design of a km^3 Mediterranean NT.

A detailed DEM of the under-water Earth surface is available from the Global Relief Data survey (ETOPO2) [56], a grid of altimetry measurements with a vertical resolution of 1 m averaged over cells of 2 minutes of latitude and longitude. In Figures 1, 2 and 3 we show the 3D maps of the areas around the three NT sites. The black curve represents the coast line, whereas the red spot stands for the location of the apparatus. By following the same approach developed in [41], we use this DEM to produce a realistic and statistically significant sample of ν_τ/τ and ν_μ/μ tracks crossing the fiducial volume of the NT that are then used to evaluate the effective aperture of each detector.

We note that when the events are reconstructed only in terms of the energy loss along the track, the UHE taus can not be distinguished from less energetic muons. This implies that the reconstruction analyses of UHE ν_μ and ν_τ events are highly entangled issues. We shall consider both of them, although for the sake of clarity we shall first

‡ This statement may not hold for exotic neutrino models [36, 37] or for peculiar astrophysical sources [38, 39, 40].

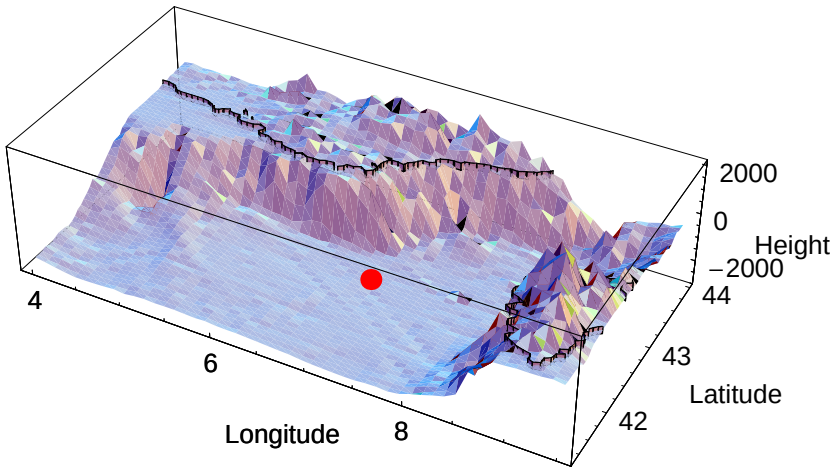

Figure 1. The surface profile of the area near the ANTARES site (red spot) at 42° 30 N, 07° 00 E. The black curve represents the coast line. The sea plateau depth in the simulation is assumed to be 2685 m. The effective volume starts at an height of 100 m from the seabed, to account for the spacing of the first photomultipliers as foresee by the current designs. The km^3 detector is oriented along the E-W/S-N directions.

focus on ν_τ detection. Of course, when considering shower events or more in general contained events—where the charged lepton production happens inside the instrumented volume—including events with peculiar topologies like "lollipop" or "double bang", there are realistic chances of flavor-tagging in the detector. However, in the UHE range above $\sim 10^7$ GeV these kind of events are subdominant with respect to the bulk of tau track-events. Further details on the flavor discrimination possibilities are discussed in Section 4.

The structure of the paper is as follows. In Section 2 we introduce the formalism and definitions used in the analysis and define the aperture for a NT. Our results for ν_τ induced events are reported and discussed in Section 3 for various incoming neutrino fluxes, while ν_μ/μ events are described in Section 4. Finally, we report our conclusions in Section 5.

2. The effective aperture of a NT

We define the km^3 NT *fiducial* volume as that bounded by the six lateral surfaces Σ_a (the subindex a=D, U, S, N, W, and E labels each surface through its orientation: Down, Up, South, North, West, and East), and indicate with $\Omega_a \equiv (\theta_a, \phi_a)$ the generic direction of a track entering the surface Σ_a. The scheme of the NT fiducial volume and two examples of incoming tracks are shown in Fig. 4. We introduce all relevant quantities with reference to ν_τ events, the case of ν_μ being completely analogous.

Let $\mathrm{d}\Phi_\nu/(\mathrm{d}E_\nu\,\mathrm{d}\Omega_a)$ be the differential flux of UHE $\nu_\tau + \bar{\nu}_\tau$. The number per unit

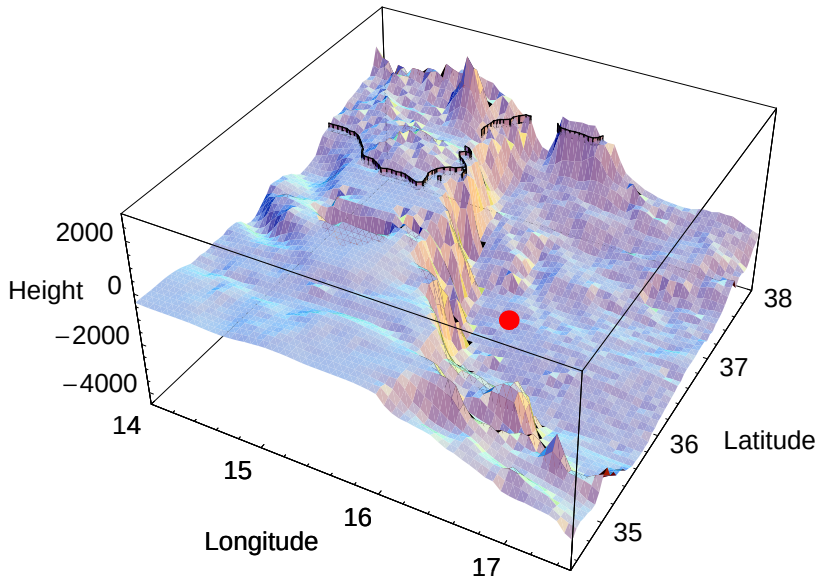

Figure 2. The surface profile of the area near the NEMO site (red spot) at 36° 21 N, 16° 10 E. The black curve represents the coast line. The sea plateau depth used in the simulation is 3424 m. The effective volume starts at an height of 100 m from the seabed, to account for the spacing of the first photomultipliers as foresee by the current designs. The km^3 detector is oriented along the E-W/S-N directions.

time of τ leptons emerging from the Earth surface and entering the NT through Σ_a with energy E_τ is given by

$$\left(\frac{\mathrm{d}N_\tau}{\mathrm{d}t}\right)_a = \int \mathrm{d}\Omega_a \int \mathrm{d}S_a \int \mathrm{d}E_\nu \, \frac{\mathrm{d}\Phi_\nu(E_\nu, \Omega_a)}{\mathrm{d}E_\nu \, \mathrm{d}\Omega_a} \times \int \mathrm{d}E_\tau \cos(\theta_a) \, k_a^\tau(E_\nu, E_\tau; \vec{r}_a, \Omega_a) \ . \quad (1)$$

This equation is the same as in [41], but for full duty cycle and detection efficiency. The kernel $k_a^\tau(E_\nu\,, E_\tau\,; \vec{r}_a, \Omega_a)$ is the probability that an incoming ν_τ crossing the Earth, with energy E_ν and direction Ω_a, produces a τ-lepton which enters the NT fiducial volume through the lateral surface $\mathrm{d}S_a$ at the position $\vec{r}_a$ with energy E_τ (see Fig. 4 for the angle definition). If we split the possible events between those with track intersecting the *rock* and the ones only crossing *water*, the kernel $k_a^\tau(E_\nu\,, E_\tau\,; \vec{r}_a, \Omega_a)$ is given by the sum of these two mutually exclusive contributions,

$$k_a^\tau(E_\nu\,, E_\tau\,; \vec{r}_a, \Omega_a) = k_a^{\tau,r}(E_\nu\,, E_\tau\,; \vec{r}_a, \Omega_a) + k_a^{\tau,w}(E_\nu\,, E_\tau\,; \vec{r}_a, \Omega_a) \ . \quad (2)$$

Let us focus on the *rock* events contributing to $k_a^{\tau,r}(E_\nu\,, E_\tau\,; \vec{r}_a, \Omega_a)$. These can be classified according to their production mechanism as follows:
1) events in which the ν_τ interacts producing a τ in the rock (r1);
2) events in which the ν_τ interacts producing a τ in water, on the way to the NT (r2);
3) events in which the ν_τ interacts producing a τ inside the NT fiducial volume (r3).

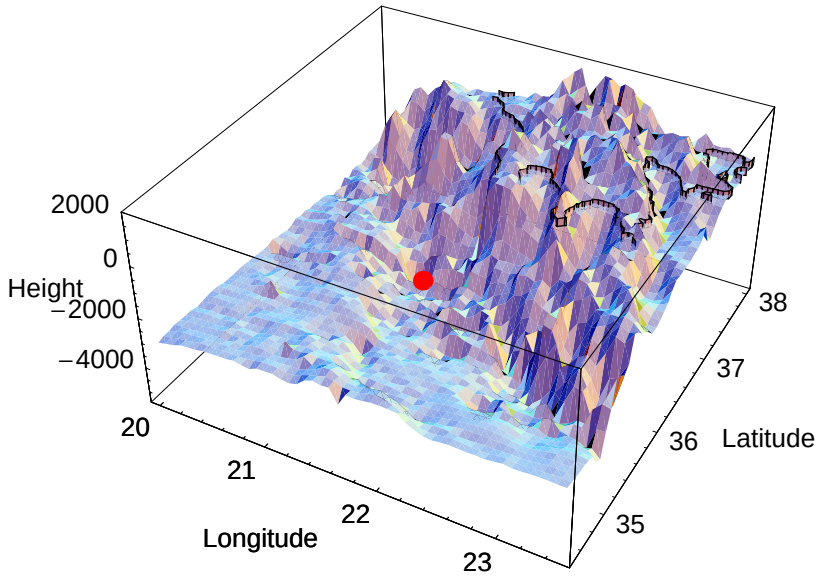

Figure 3. The surface profile of the area near the NESTOR site (red spot) at 36° 21 N, 21° 21 E. The black curve represents the coast line. The sea plateau depth in the simulation is assumed to be 4166 m. The effective volume starts at an height of 100 m from the seabed, to account for the spacing of the first photomultipliers as foresee by the current designs. The km^3 detector is oriented along the E-W/S-N directions.

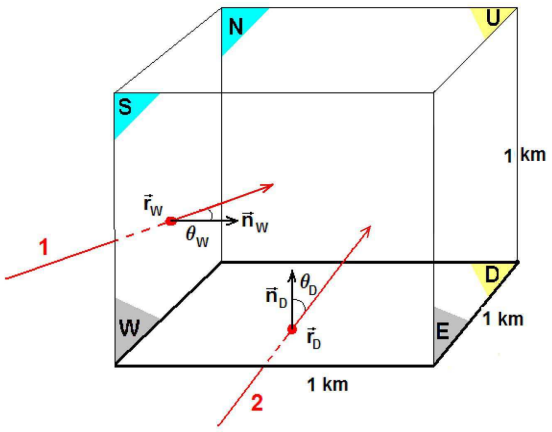

Figure 4. The angle definition and the fiducial volume of a km^3 NT.

Therefore one has

$$k_a^{\tau,r}(E_\nu\,,E_\tau\,;\vec{r}_a,\Omega_a) = k_a^{\tau,r1}(E_\nu\,,E_\tau\,;\vec{r}_a,\Omega_a) + k_a^{\tau,r2}(E_\nu\,,E_\tau\,;\vec{r}_a,\Omega_a) + k_a^{\tau,r3}(E_\nu\,,E_\tau\,;\vec{r}_a,\Omega_a)\ . \tag{3}$$

Although here, for the sake of brevity, we only discuss in details the events occurring in rock (r1), the analysis of those of type (r2) and (r3) is completely analogous and

straightforward. Of course, all contributions (r1)-(r3) have been added to compute the event rate.

As already shown in details in [41, 53] a (r1)-event corresponds to the simultaneous fulfillment of the following conditions:

1) A ν_τ with energy E_ν travels over a distance z through the Earth before interacting. The corresponding probability P_1 is given by

$$P_1 = \exp\left\{-\frac{z}{\lambda^\nu_{CC}(E_\nu)}\right\} \ , \tag{4}$$

where

$$\lambda^\nu_{CC}(E_\nu) = \frac{1}{\sigma^{\nu N}_{CC}(E_\nu)\, \varrho_r\, N_A} \ , \tag{5}$$

where N_A the Avogadro number. See [41, 53] for notations as well as a detailed discussion of the neutrino-nucleon cross section, $\sigma^{\nu N}_{CC}(E_\nu)$. In the present formalism the effect of the Earth density profile is approximated using, track by track, the averaged ϱ_r along the chord subtended by that track. The calculations are made with the parametrization of the Earth density profile of Ref. [57]. Note, however, that for almost horizontal events particles travel in the terrestrial crust only, and thus the superficial value for the Earth density $\varrho_r \simeq 2.65$ g/cm^3 [51] would be an accurate approximation. Some differences could appear for low energy particles deeply crossing the Earth. We checked that, using the constant value of the crust density for all the Earth density profile the changes in the tau aperture are generally less than 10%, while the effect is of the order of 16% for muons with E $< 10^5$ GeV, i.e. below the energy range for which the cosmic flux is expected to dominate over the atmospheric flux. The inclusion of the Earth density profile also affect at the 10% level the distributions of both τs and μs incoming zenith angles: due to increased screening along the nadir direction (vertical up-going), the distributions slightly shrink along the horizontal direction.

2) The neutrino produces a τ in the interval $z, z + \mathrm{d}z$, the probability of such an event being

$$P_2\, \mathrm{d}z = \frac{\mathrm{d}z}{\lambda^\nu_{CC}\,(E_\nu)} \ . \tag{6}$$

We do not consider here the event corresponding to the scattering of a ν_τ via neutral current in the Earth followed by conversion via charged current, which amounts to a small distortion of the incoming neutrino flux, the latter being yet unknown [59]. Of course, this sub-leading effect should be added when trying to reconstruct the flux from experimental data. Also, we consider the charged lepton track as collinear with the parent neutrino direction, which is highly accurate given the huge relativistic boosting factors involved.

3) The produced τ emerges from the Earth rock with an energy E'_τ. This happens with a probability

$$P_3 = \exp\left\{-\frac{m_\tau}{c\tau_\tau \beta_\tau \varrho_r}\left(\frac{1}{E'_\tau} - \frac{1}{E^0_\tau(E_\nu)}\right)\right\}$$

$$\times\, \delta\left(E'_\tau - E^0_\tau(E_\nu)\, e^{-\beta_\tau \varrho_r (z_r - z)}\right) \ , \tag{7}$$

where $m_\tau = 1.78$ GeV, $\tau_\tau \simeq 3.4 \times 10^{-13}$ s is the τ mean lifetime and E^0_τ is the τ energy at production, whereas the parameter $\beta_\tau = 0.71 \times 10^{-6}$ cm^2 g^{-1} weights the leading term in the τ differential energy loss in rock [53, 60],

$$\frac{\mathrm{d}E_\tau}{\mathrm{d}z} = -\left(\beta_\tau + \gamma_\tau E_\tau\right) E_\tau \varrho_r \ . \tag{8}$$

The contribution of γ_τ can be neglected as it only affects extremely energetic τ's which, differently from the case of the Pierre Auger Observatory, are not relevant for NT's. The quantity $z_r\left(\vec{r}_a\,, \Omega_a\right)$ represents the total length in rock for a given track entering the lateral surface Σ_a of the fiducial volume at the point $\vec{r}_a$ and with direction Ω_a.

4) Finally, the τ lepton emerging from the Earth rock propagates in water and enters the NT fiducial volume through the lateral surface Σ_a at the point $\vec{r}_a$ with energy E_τ. The corresponding survival probability is

$$P_4 = \exp\left\{-\frac{m_\tau}{c\tau_\tau \beta_\tau \varrho_w}\left(\frac{1}{E_\tau} - \frac{1}{E'_\tau}\right)\right\} \delta\left(E_\tau - E'_\tau\, e^{-\beta_\tau \rho_w z_w}\right) \ , \tag{9}$$

where ϱ_w stands for the water density and $z_w\left(\vec{r}_a\,, \Omega_a\right)$ represents the total length in water before arriving to the fiducial volume for a given track entering the lateral surface Σ_a at the point $\vec{r}_a$ and with direction Ω_a.

Collecting together the different probabilities in Eqs. (4), (6), (7) and (9), we have

$$k^{\tau,r1}_a(E_\nu\,, E_\tau\,; \vec{r}_a, \Omega_a) = \int_0^{z_r} \mathrm{d}z \int_0^{E^0_\tau(E_\nu)} \mathrm{d}E'_\tau \ P_1\, P_2\, P_3\, P_4 \ . \tag{10}$$

Similar results can be obtained for the (r2)- and (r3)-events as well as for those we defined as *water*-like.

For an isotropic flux we can rewrite Eq. (1), summing over all the surfaces, as

$$\begin{aligned} \frac{\mathrm{d}N^{(r,w)}_\tau}{\mathrm{d}t} &= \int \mathrm{d}E_\nu \ \frac{1}{4\pi} \frac{\mathrm{d}\Phi_\nu(E_\nu)}{\mathrm{d}E_\nu} A^{\tau(r,w)}(E_\nu) = \\ &= \sum_a \int \mathrm{d}E_\nu \ \frac{1}{4\pi} \frac{\mathrm{d}\Phi_\nu(E_\nu)}{\mathrm{d}E_\nu} A^{\tau(r,w)}_a(E_\nu) \ , \end{aligned} \tag{11}$$

which defines the total aperture $A^{\tau(r,w)}(E_\nu)$, with "r" and "w" denoting the *rock* and *water* kind of events, respectively. The contribution of each surface to the total aperture reads

$$A^{\tau(r,w)}_a(E_\nu) = \int \mathrm{d}E_\tau \int \mathrm{d}\Omega_a \int \mathrm{d}S_a \ \cos\left(\theta_a\right) \ k^{\tau,(r,w)}_a(E_\nu\,, E_\tau\,; \vec{r}_a, \Omega_a) \ . \tag{12}$$

3. The event rate for ν_τ interactions

We show in Fig. 5 the apertures $A^{\tau(r,w)}$ for the NEMO site together with the corresponding quantity for the Pierre Auger Observatory Fluorescence Detector (FD) calculated in [41].

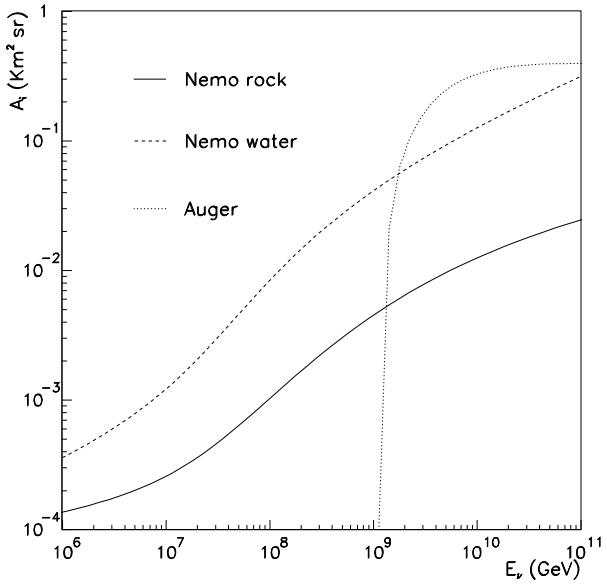

Figure 5. The effective apertures $A^{\tau(r)}(E_\nu)$ (solid line) and $A^{\tau(w)}(E_\nu)$ (dashed line) defined in Eq. (11) versus tau neutrino energy for NEMO. The dotted line corresponds to the same quantity for the Auger Fluorescence Detector for Earth-skimming ν_τ as in [41].

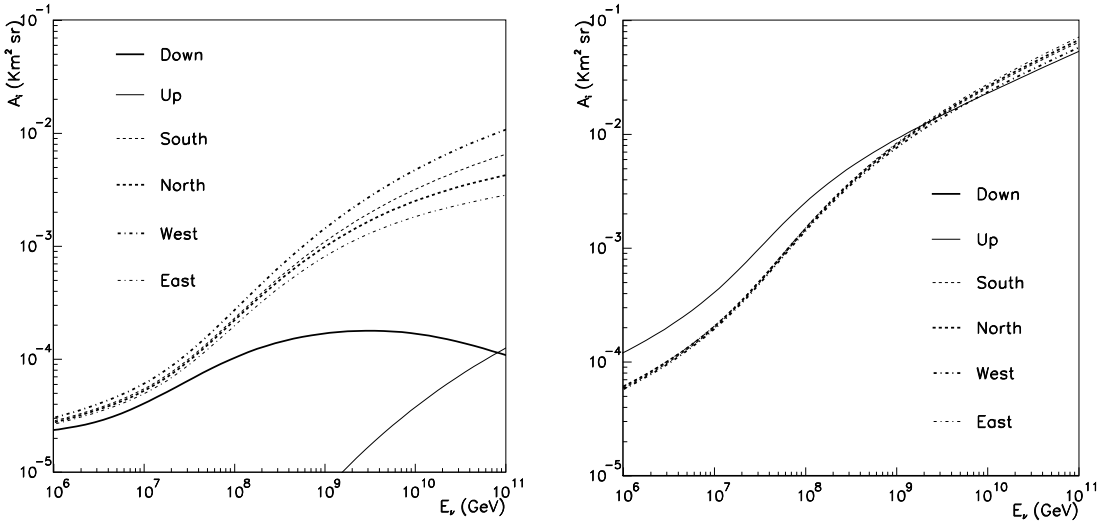

Figure 6. The effective apertures $A_a^{\tau(r,w)}(E_\nu)$ of Eq. (12) versus tau neutrino energy for (left) *rock* events and (right) *water* events for the NEMO site.

Note that the Auger case is only for Earth-skimming τ's, since down-going neutrino induced events can be disentangled from ordinary cosmic rays only for very inclined showers. Interestingly, the NEMO-*water* and Auger-FD apertures almost match at the FD threshold of 10^{18} eV, so that using both detectors results into a wide energy range of sensitivity to ν_τ fluxes.

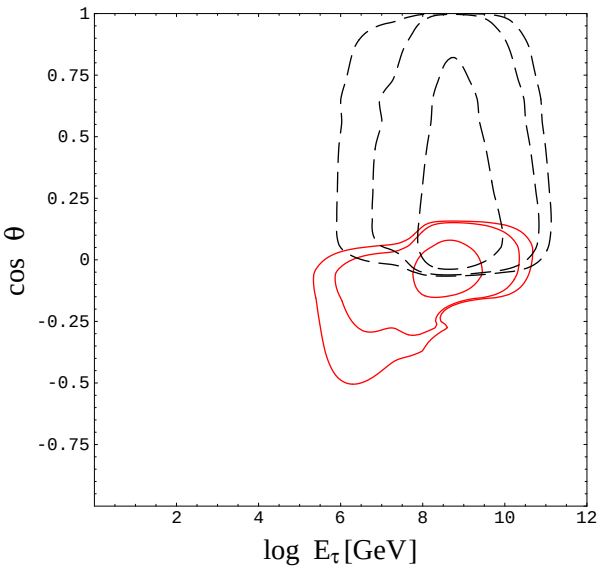

Figure 7. Contour plot in the plane zenith angle-τ energy for the NEMO site and for *rock* (red full lines) and *water* (black dashed lines) events. In both cases the contours enclose 68, 95 and 99 % of the total number of events calculated assuming a GZK-WB flux ([61], see also [55]). $\cos\theta = 1, 0, -1$ correspond respectively to down-going, earth-skimming, and up-going events.

We show in Fig. 6 the high energy behavior for each surface contributing to the effective aperture. For *rock* events there is a clear W-E asymmetry, easily understood in terms of matter effects related to the particular morphology of the NEMO site (see Fig. 2). A much smaller S-N asymmetry is also present. In other words, the asymmetries in the number of rock-events reflect the asymmetries in the morphology of the site.

For neutrino energies larger than 10^7 GeV the main contribution to the aperture $A^{\tau(r)}(E_\nu)$ comes from the lateral surfaces, i.e. from τ leptons emerging from the rock far from the NT basis and crossing the fiducial volume almost horizontally. Instead, the upper surface contribution is negligible due to the very small fraction of events crossing the rock and entering the detector from above. The decreasing contribution of the bottom face to rock events is due to the Earth shadowing effect.

For *water* events the contribution to the aperture from all surfaces is comparable (except for the lower one which has no events), the upper one providing a slightly larger contribution as the energy decreases. Indeed, events which would cross the lateral surfaces should travel over a longer path in water and this becomes more unlikely at lower energies due to the shorter τ decay length. The matter effect in the case of *water* events is less pronounced and anticorrelated with the asymmetries in the morphology of the site resulting effectively in a small (percent) screening effect.

In Fig. 7 we report, for both the *rock* and *water* cases and for the NEMO site, the contours enclosing 68, 95 and 99 % of the total event rate, as they appear in the plane E_τ-θ plane, where θ is the arrival direction zenith angle. These results were

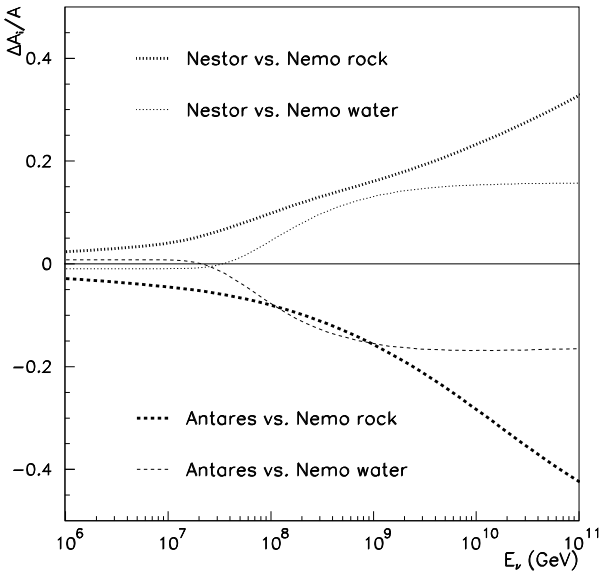

Figure 8. A comparison of the effective apertures $A^{\tau((r,w))}(E_\nu)$ for the three NT sites. We plot the ratios $[A^{\tau((r,w))}(\texttt{NESTOR}) - A^{\tau((r,w))}(\texttt{NEMO})]/A^{\tau((r,w))}(\texttt{NEMO})$ and $[A^{\tau((r,w))}(\texttt{ANTARES}) - A^{\tau((r,w))}(\texttt{NEMO})]/A^{\tau((r,w))}(\texttt{NEMO})$ versus the neutrino energy.

obtained assuming a Waxmann-Bahcall-like neutrino flux (GZK-WB) [61] (see also [41] and references therein). As the energy increases, the arrival directions of *rock* events are almost restricted to the horizontal (Earth-skimming), while at lower energies the earth-screening effect is less pronounced and this explains the broader angular distribution. The situation is different for *water* events for which the angular distribution is broad at all energies, a purely geometrical effect due to the fact that (down-going) *water* events are not screened in few kilometers of water. The same geometrical considerations explain the ratio of *water* to *rock* event rate of $\mathcal{O}(10)$ (see Table 1) which is simply related to the ratio of down-going to Earth-skimming solid angles. This is the same kind of behavior expected in the Auger detector although, as we already mentioned, the down-going events in this case are hardly distinguishable from the background of proton-induced showers so that only Earth-skimming or almost horizontal showers can be used to identify unambiguously the neutrino-induced events. It is also worth commenting the expected τ energy distribution shown in Fig. 7. All events correspond to a relatively narrow energy window, from 10^6 GeV up to 10^{10} GeV, where the lower cut-off arises from the shorter τ decay length at low energy.

In Fig. 8 we compare the detection performances of a km^3 NT placed at one of the three sites in the Mediterranean sea. The NESTOR site shows the highest values of the τ-aperture for both *rock* and *water*, due to its larger depth and the particular matter distribution of the surrounding area, while the lowest rates are obtained for ANTARES. The aperture in the three sites can be quite different at high energy, but in order to get the expected number of UHE events per year, one has to convolve the aperture with a

Surf.	ANTARES	NEMO	NESTOR
D	0.0059/0	0.0059/0	0.0058/0
U	0/0.1677	0.0002/0.2133	0.0002/0.2543
S	0.0185/0.1602	0.0256/0.1773	0.0240/0.2011
N	0.0241/0.1540	0.0229/0.1823	0.0321/0.1924
W	0.0212/0.1584	0.0335/0.1691	0.0265/0.2002
E	0.0206/0.1589	0.0190/0.1875	0.0348/0.1907
Total	0.090/0.799	0.107/0.929	0.123/1.039

Table 1. Estimated rate per year of *rock/water* τ events at the three km^3 NT sites for a GZK-WB flux ([61, 55]). The contribution of each detector surface to the total number of events is also reported.

neutrino flux which typically drops rapidly with the energy. Although the percentage value of the matter effects remains unchanged, in this very low statistics regime they can be hardly distinguished; still, they can be enhanced by an appropriate choice of the detector shape as we discuss in the following.

Knowing the aperture of the NT at each site, we can compute the expected τ event rate, once a neutrino flux is specified. In Table 1 these rates are shown assuming a GZK-WB flux ([61, 55]). The effect due to the local matter distribution is responsible for the N-S, W-E and NE-SW asymmetries for the ANTARES, NEMO and NESTOR sites, respectively, as expected from the matter profiles shown in Figs. 1, 2 and 3. These matter effects, for the specific UHE flux considered (GZK-WB), correspond to an enhancement of *rock* events which goes from 20 to 50% for the three sites, respectively, and a screening factor for *water* events from 3 to 10%. The largest relative difference among lateral surfaces is in the case of W/E for NEMO, where the huge wall to the west of the site (see Fig. 2) improves the rate by about 75%, almost a factor 2! Notice also that the *water* events from the U surface are basically proportional to the depth.

It is important to emphasize that the impact of matter effects on the rates depends critically upon the energy spectrum of the UHE neutrino flux. For more energetic neutrino fluxes the enhancement factor is expected to be more significant (see the energy behavior of $A_a^{\tau(r)}(E_\nu)$ in Fig. 6). In Table 2 the rate of *rock/water* τ events are computed for the three different km^3 NT sites using several UHE neutrino fluxes as already considered in [41, 53] and described in [61]-[67] (see also Fig. 11). For comparison, we also show in the last column the corresponding prediction for Earth-skimming ν_τ at Auger-FD. As can be seen from Table 2, the relative enhancements due to matter effects on *rock* events can be as large as 30%, whereas the difference in the rates of *water* events for a fixed neutrino flux is mainly due to the different depth of the three sites.

An interesting feature is the dependence of the event rate upon the shape of the NT detector for a fixed total volume of 1 km^3, a property that might be relevant for the eventual design of the detector. Consider for example a km^3 NT placed at the NEMO site with the shape of a parallelepiped rather than a cube, where in particular

ν-fluxes	ANTARES	NEMO	NESTOR	Auger-FD [41]
GZK-WB	0.090/0.799	0.107/0.929	0.123/1.039	0.074
GZK-L	0.099/1.076	0.130/1.282	0.157/1.465	0.213
GZK-H	0.225/2.744	0.313/3.280	0.386/3.766	0.560
NH	0.891/8.696	1.102/10.19	1.295/11.47	1.245
TD	0.701/5.072	0.817/5.799	0.921/6.424	0.548

Table 2. Yearly rate of *rock/water* τ events at the three km^3 NT sites for different UHE neutrino fluxes. GZK-H is for an initial proton flux $\propto 1/E$, assuming that the EGRET flux is entirely due to π- photoproduction. GZK-L shows the neutrino flux when the associated photons contribute only up to 20% in the EGRET flux. GZK-WB stands for an initial proton flux $\propto 1/E^2$ [61]–[65]. The other two neutrino fluxes correspond to more exotic UHECR models. NH represents the neutrino flux prediction in a model with new hadrons [66], whereas TD is the neutrino flux for a topological defect model [67]. In the last column we report the corresponding prediction for Earth-skimming ν_τ at Auger-FD.

the E and W surfaces are enlarged by a factor 3 in the horizontal dimension, the N and S surfaces being reduced by the same factor, keeping the height of towers still of 1 km. In this case the expected rate of *rock* events per year is enhanced by almost a factor 2, from 0.11 to 0.18 for the GZK-WB flux, while this enhancement could be even larger for neutrino fluxes with a larger high energy component. Moreover, the expected rate of *water* events increases as well by a factor of the order of 50%, from 0.93 up to 1.40 per year. Similar exercises can be also performed for the ANTARES and NESTOR sites. Of course, a further possibility which might favor UHE-τ detection consists in increasing the effective volume of the detector keeping unchanged the 1 km height and the number of towers of photomultipliers but adopting a larger spacing. As an example, for a factor four larger volume with a doubling of the tower spacing both the *rock* and *water* τ events would increase by almost a factor two, but obviously at the expense of the energy threshold and the quality of the event reconstruction for "low-energy" (TeV) neutrinos. For a detector aiming at the exploration of the range above the PeV, this is a less severe problem.

The fact that the event rate depends upon the total surface of the detector is a peculiar feature of a NT, quite differently from what expected at the Auger observatory. Actually, in this case observed showers are generally initiated not very far from the detector compared to its dimensions so that the shape of the detector (i.e., the position on the border where the FDs are placed) is not as important as its "volume" (controlled by the area enclosed by the FDs). In fact, in order to produce a τ emerging from the Earth with enough energy to generate a shower detectable by the Auger FDs, the energy of the neutrino should be larger than 1 EeV$= 10^{18}$ eV, taking into account the τ energy loss in the rock. But the decay length of such a UHE τ is $l_{\rm decay} \simeq 50\,{\rm km} \times (E_\tau/{\rm EeV})$, to be compared with the dimensions of the Auger fiducial volume, $\sim 50 \times 60 \times 10$ km^3. Conversely, a neutrino telescope can detect taus or muons which are produced very far

from the detector by a neutrino charged-current interaction, from distances comparable to the charged lepton range at that particular energy [31]. Indeed, the τ range in water is of the order of several kilometers: from the value of $\beta_\tau = 0.71 \times 10^{-6}$ cm^2 g^{-1} we obtain an attenuation length $1/(\beta_\tau \varrho_w) \simeq 15$ km, while for muons (see next section) the range is approximately eight times smaller, of the order of 2 km. In other words, the effective volume of a NT of the kind discussed so far can be much larger than 1 km^3, thus maximizing the detector area might greatly improve the detection rate.

Of course, one should not forget that the design of a NT also depends strongly upon more detailed experimental considerations. Shapes which are not very compact or a detector with very sparse instrumentation have worse performances in the reconstruction of track properties as well as in signal-background separation, though this is mainly problematic at energies lower than 100 TeV, in the atmospheric neutrino energy range. In any case, our analysis suggests that the choice of the detector shape could be an important feature in orienting the target of a NT investigation towards either atmospheric or extra-atmospheric neutrino physics. In this respect, the possibility to modify this parameter quite easily for a NT water detector offers a great advantage with respect to an under-ice detector.

A comment is in turn regarding the various approximations we used in the calculation. In particular we neglected tau regeneration effects. It is well known that these effects depend on the adopted incoming spectrum with a typical behavior in which the steeper the spectrum the less relevant the effect is [58, 34]. For an E^{-2} spectrum the effect is almost negligible [58], while for harder spectra like the ones we presently consider the effect can be of the order of 20% for taus coming from the nadir direction and of decreasing relevance for more horizontal events [34]. An estimate of the direction averaged effect gives then a correction less of 10%.

A further approximation regards the stochastic nature of the tau interaction in matter that we approximated like a continuous energy loss process through the parametrization of Eq. (8). At energies larger than 10^6 GeV, tau energy losses are affected by the large theoretical uncertainty on cross-section for photonuclear interaction, the leading mechanism at these energies (see [53] and [72], and references therein). Differently from muons, for taus the dominant source of uncertainty is not the stochastic vs. continuous nature of the energy loss, but the model-dependence of the photonuclear interaction itself; the stochastic nature of the losses is then sub-dominant with respect to the understanding of the process. A detailed discussion of the problem is given in Ref. [53]. The continuous approximation is then enough for the estimate of the mean rate values as given in the text, especially for a relative comparison of the sites. A more careful treatment would be needed if one is interested in a realistic estimate of the errors.

A final comment deserves the dependence that matter effects could have not only on truly differences of amount of matter present in different directions, but also on the differences in the lepton interactions in water or rock due to the different chemical composition (A, Z), i.e. to differences between β_r and β_w. We study the issue performing

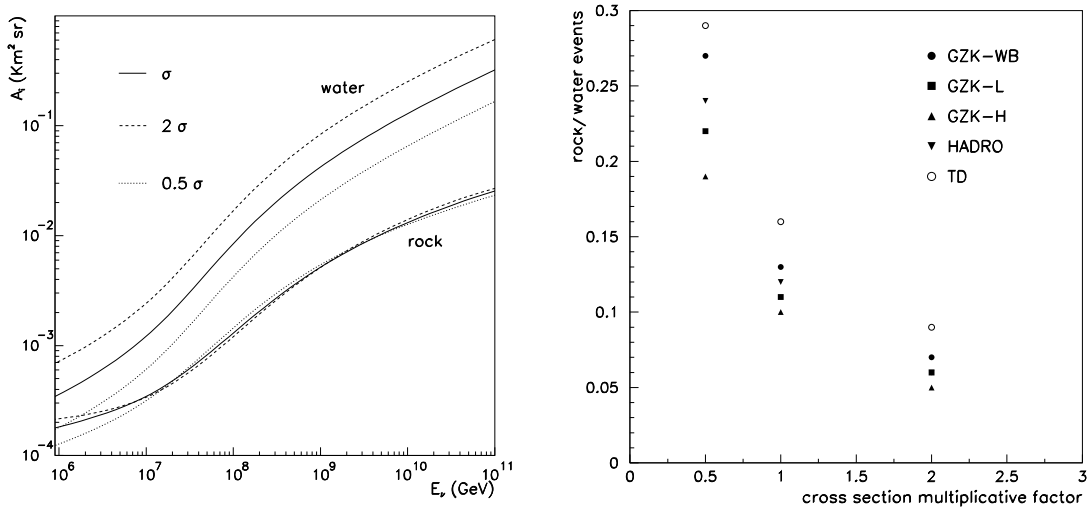

Figure 9. (Left) The effective apertures $A^{\tau(r,w)}(E_\nu)$ for the NEMO site for a ν_τ–nucleon cross section multiplied by a factor 0.5, 1 and 2 with respect to the standard result σ. (Right) Ratios of the number of events in *rock/water* when the cross section is rescaled by the factor shown on the x axis, for several incoming UHE neutrino fluxes.

detailed calculations of the lepton propagation as given in [73]. The calculations show that the (A,Z) dependence is of the order 10% for taus, almost constant at high energies (> 1 PeV), while of the order 20% for muons again almost constant at high energies. Given the model uncertainties in the tau losses and the level of approximation of 10% used throughout the paper we used the same value of β for rock and water losses for both muons and taus so that the differences seen at high energies in the apertures in Fig.6 has to be all ascribed to a genuine matter effect. Note moreover that the matter effect is a feature increasing with energy, amounting for example in a factor even of four in difference between the $W - E$ surfaces for NEMO at 10^{11} GeV, while the percentage difference in β_w/β_r always remain of the order 10% through the whole energy range. The role of chemical composition then is at most subdominant.

One of the main motivations for studying UHE neutrinos is that they provide a possibility to explore a range of energies for scattering processes which is still untested (maybe impossible to test) by particle accelerators. In this respect, measuring the neutrino–nucleon cross sections at high energies could have a large impact on constraining or discovering new physics beyond the standard model (see e.g. [30, 68]). While a measurement of the event energy spectrum cannot remove in general a degeneracy between the neutrino cross section and the incoming neutrino flux, a neutrino telescope could offer the interesting capability of disentangling these two factors because of the role of matter effects. Indeed, provided that enough statistics is collected and the detector has a good zenith angle resolution, the flux dependence can be subtracted off by measuring the ratio of the event rates coming from different directions [69, 70, 71]. In the left panel of Fig. 9 we show how the NEMO effective apertures for τ *rock* and

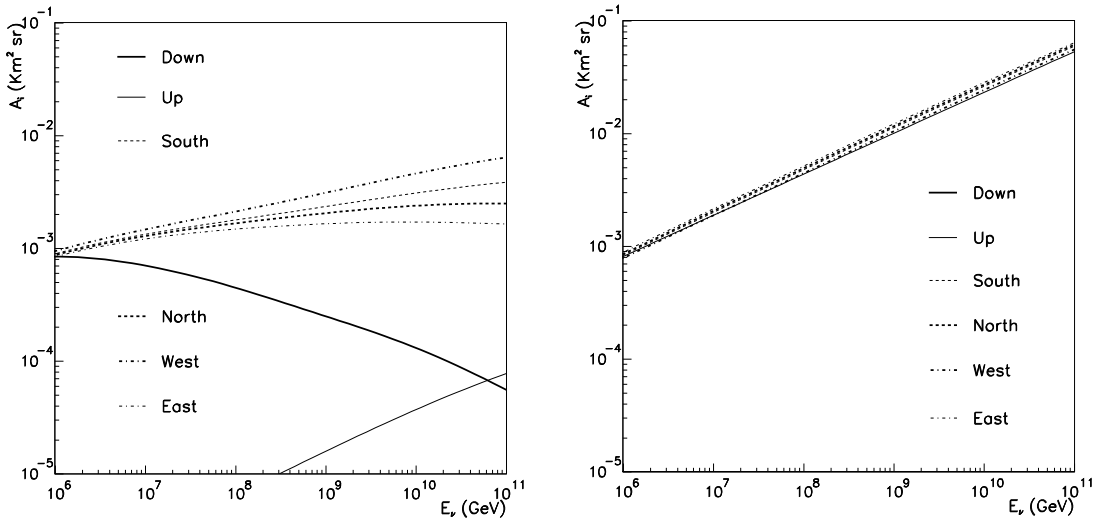

Figure 10. The effective apertures $A_a^{\mu(r,w)}(E_\nu)$ versus the muon neutrino energy for (left) *rock* events and (right) *water* events at the NEMO site.

water events change if the neutrino-nucleon cross section is half or twice the standard model result, while in the right panel we display the ratio of *water/rock* τ event rates for several adopted fluxes. We see that this ratio is quite sensitive to the value of the cross section. In particular, the number of *rock* events is essentially unaffected while the *water* event rate increases almost linearly with the cross section. Clearly, since the statistical error on the ratio would be dominated by the rare *rock* events, an experiment which aims at exploiting this effect should maximize the acceptance for almost horizontal events. We conclude by noticing that our results do not take into account any detailed experimental setup and up to this point the ν_μ contribution is not yet considered. Nevertheless, since both the incoming neutrino flux and cross section on nucleons are expected to be flavor independent the possibility of determining both these quantities at a NT seems an interesting perspective. A more detailed analysis of this issue will be addressed elsewhere.

4. The ν_μ contribution: disentangling μ's from τ's

In the previous Section we have discussed the rate of ν_τ events implicitly assuming that a τ lepton can be distinguished from a μ in a NT. However, given the experimental characteristics of the detector, this could be a difficult task and ν_μ events should be also included in any realistic simulation. We address this issue in the present Section.

Using the definition of the aperture in full analogy with Eq. (12) and applying the same considerations of Section 2 to ν_μ/μ, we have computed the μ apertures for *water* and *rock* events for the various surfaces of the NT, adopting the value $\beta_\mu = 0.58 \times 10^{-5}$ cm^2 g^{-1} in the expression of the muon differential energy loss analogous to Eq. (8) (as for the τ, the term weighted by γ_μ is negligible for the energy range of interest). The

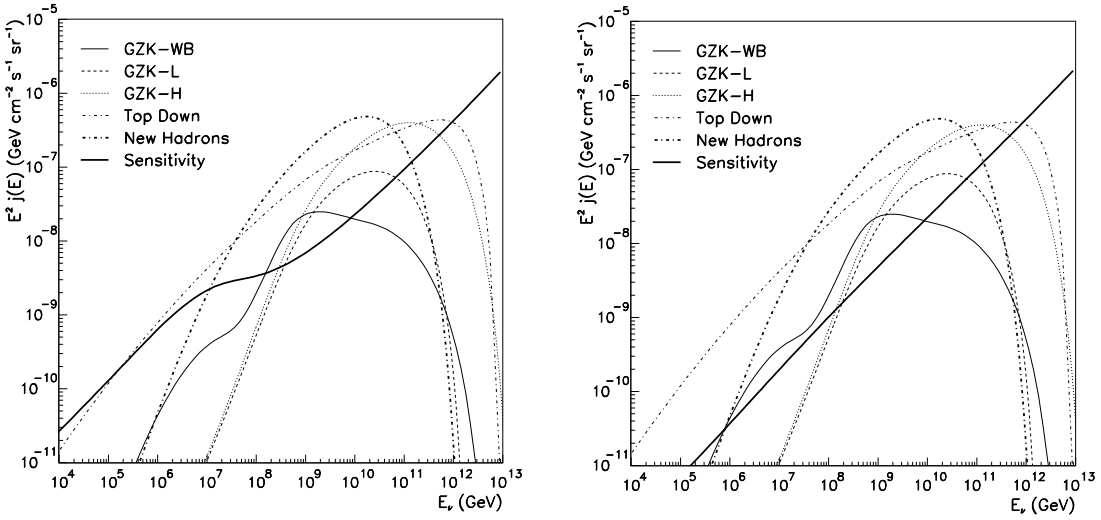

Figure 11. The total NEMO sensitivities for (left) τ and (right) μ events versus the neutrino energy, compared with the UHE neutrino fluxes considered in the paper.

results are shown in Fig. 10. The main features as well as the role of matter effects are essentially unchanged for muons, the only difference coming from the muon contribution at lower energies because of the longer muon lifetime compared to that of taus.

It is worth to discuss briefly the adopted parametrization for the muon energy losses. As discussed above, tau energy losses are affected by the large theoretical uncertainty on cross-section for photonuclear interaction. On the other hand, photonuclear interactions are less relevant for muon propagation, thus the theoretical uncertainty on the energy loss is correspondingly smaller. We then checked the validity of the approximation given in Section 4 versus the detailed calculation given in [73]. We found that the accuracy is at the level of 15% over the whole energy range. The impact of this uncertainty on the expected event rate is as follows: a 15% increase of β_μ gives a few % decrease of the number of water events and a $\sim$ 10 % decrease of the number of rock events. This uncertainty then does not affect the estimate of the number of ν_μ events while a more careful treatment is required for a reliable forecast of the neutrino cross-section sensitivities at a Neutrino Telescope.

In Fig. 11 we summarize the τ and μ results by showing the total sensitivity $S^{\mu,\tau}$ for NEMO defined as $S^{\mu,\tau}\, E_\nu\, A^{\mu,\tau} = 1$ event year^{-1} (E_ν decade)$^{-1}$, with $A^{\mu,\tau}$ the total μ and τ effective aperture, respectively; we also show the various neutrino fluxes considered through the paper. We see that in agreement with the results of Table 2, at least one event per year is expected even in the case of a GZK-WB flux, while larger rates are expected for higher fluxes (see also [74]). Notice that in the energy bin $10^8 - 10^{10}$ GeV both μ and τ contributions are comparable while muons are expected to dominate in the lower energy range, depending on the particular flux we consider.

Concerning the possibility to distinguish between UHE taus and less energetic muons a comment is in turn. As we mentioned in the Introduction, the main difficulty

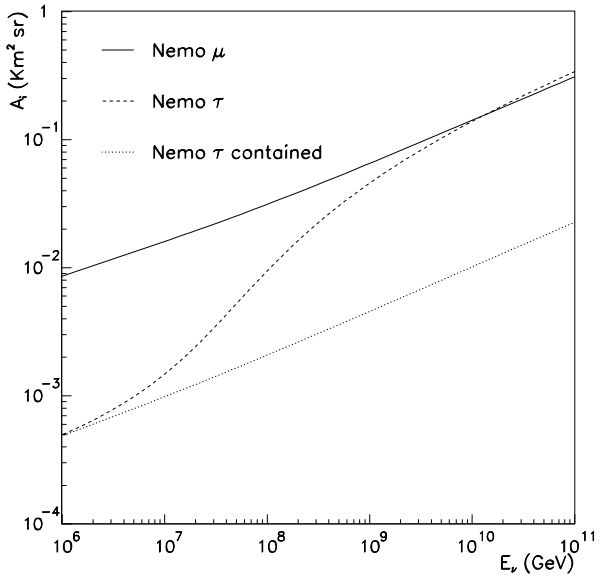

Figure 12. Total τ, μ and contained events apertures for the NEMO site. Note that the contained events are the same for all neutrino flavors.

is that Cherenkov detectors like a NT do not measure the particle energy but rather the energy loss inside the detector volume and thus a high-energy τ tracks can be misidentified with a muon track of lower energy. This is because the ratio of τ to μ energy loss rate is given by $\beta_\tau/\beta_\mu \simeq 1/8$. In principle, given that tau energy losses are dominated by photonuclear processes versus radiative interactions for muons, it would be possible to distinguish a muon-track from a tau-track from the different hadronic content along the track. However, Montecarlo simulations indicate that NT's are poorly sensitive to this signature [34].

As far as the contained events are concerned (i.e. where the charged lepton production happens inside the instrumented volume), the telescope has, instead, realistic chances of flavor-tagging. As long as the energy-loss or decay range of the particle to be detected is small compared with the detector size, the event rate depends basically on the fiducial volume. This is always the case for neutral current events, which if detectable produce a localized hadronic shower from the struck nucleon, and for charged current ν_e-events, since the electron rapidly loses its energy. On the contrary, for energies above the TeV scale, ν_μ's charged current events produce muons which are detectable as tracks several km away from the production point. The case of ν_τ charged current events is yet different: for energies $\lesssim 10^7$ GeV, the boosted decay range of the tau particle is negligible with respect to the detector size and depth, and the event rate is determined by the instrumented volume, like for ν_e-events. On the other hand, for the typical spacings between strings/photomultipliers considered by current designs, above the PeV scale the boosted τ decay length is larger than the spacing and one starts resolving the *tracks*, while below this energy τ produce showers which differ from ν_e-events only by

the hadronic content, which is however challenging to tag.

We show in Fig. 12 the total apertures for τ and μ events at the NEMO site together with the aperture for τ contained events (the same would apply for μ contained events). Indeed, contained events represent a sub-leading although non-negligible fraction of the total number of events, always of the order of 10% for μ and even greater for low energy τ ($\lesssim 10^7$ GeV) due to the very short ($\lesssim 1$ km) decay length at these energies. Moreover, the contained aperture depends only on the neutrino interaction probability so that it can be considered also a reliable estimate of the e-induced showering events, neglecting the effect of the Glashow $\bar{\nu}_e e^-$ resonance at 6.3 PeV. It may also be possible to identify *lollipop* events in which a τ with energy larger than PeV produces a long minimum-ionizing track that enters the detector and eventually ends in a huge burst as the τ lepton decays into a final state with hadrons or an electron. In this case, the final burst would be a direct measurement of the τ energy while the energy loss along the track would be smaller than for a muon of the same energy. Probably, the cleanest signature of a τ particle would be the detections of a double-bang event [75] in which a ν_τ interacts inside the detector and the produced τ decays in shower again in the detector, but the probability of such an event is extremely small. In any case, all these possibilities suffer from lower statistics as they all require that the interactions (showering or production) occur inside the detector, with a reduction of the effective volume down to 1 km^3 compared with the several km^3 effective volume for μ and τ events which go across the NT fiducial volume.

In view of these considerations, we conclude that, at least for the bulk of the events, the most viable strategy is to combine both muon and tau contributions and construct spectra depending upon quantities which are directly observable. The simplest choice is to consider the energy loss rate inside the detector which amounts to measure the track length and the total deposited energy and the arrival direction. In Fig. 13 we show the contours of expected μ and τ event rates in terms of the zenith angle of arrival directions and $\mathrm{d}E/\mathrm{d}x \simeq -\beta E \varrho_w$. For relatively low energy losses $\beta E \varrho_w \lesssim 10^5\,\mathrm{GeV/km}$ the whole dominant contribution comes from muons, which therefore can be easily disentangled, whereas in the high energy loss tails the event distributions are almost the same for both neutrino flavors and one is forced to use the total $\nu_\mu + \nu_\tau$ events as the input of any analysis of the data.

5. Conclusions

Ultra-high energy neutrinos represent one of the main targets for several experiments which adopt a variety of detection techniques. Among these, the optical Cherenkov neutrino telescopes deployed under water or ice look for the tracks of charged leptons produced by the high energy neutrinos that reach the Earth. In this paper, we have presented a new study of the performance of a km^3 neutrino telescope to be located in any of the three sites in the Mediterranean sea proposed by the ANTARES, NEMO, and NESTOR collaborations. Our main goal is to compare the performances of the different

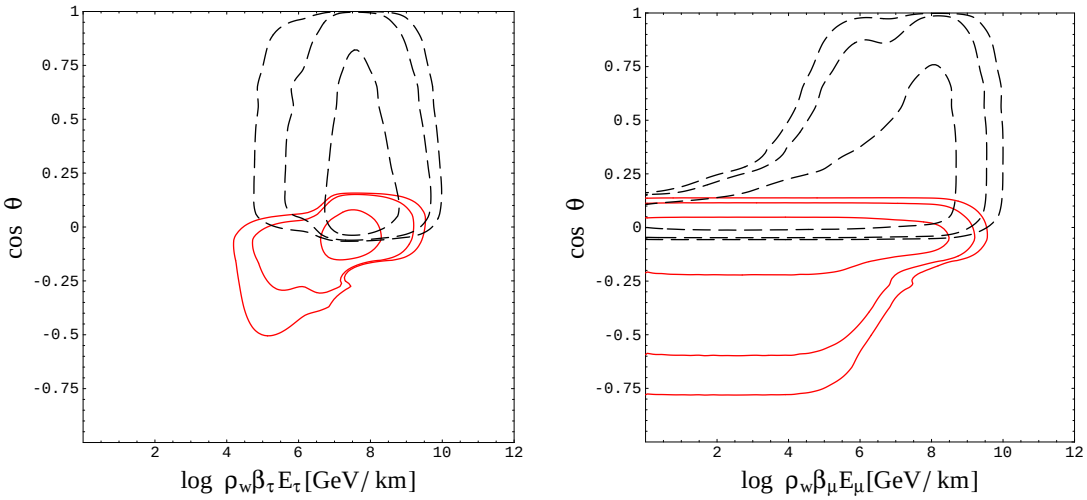

Figure 13. Contour plots of the number of *rock* events (red full lines) and *water* events (black dashed lines) at the NEMO site in the zenith angle-dE/dx plane for τ (left panel) and μ (right panel) assuming a GZK-WB neutrino flux. The contours enclose 65, 95 and 99 % of the total number of events.

sites, keeping apart detector-specific features, like partial detection efficiency or the architecture adopted for the towers of strings. We concentrated instead on the details of the under-water surface profile of each of the three sites, using the data from a Digital Elevation Map. By generating a realistic and statistically significant sample of ν_τ/τ and ν_μ/μ tracks crossing the fiducial volume of the km^3 neutrino telescope, we have calculated its effective aperture to UHE ν_τ and ν_μ neutrinos and the expected number of events for different UHE neutrino fluxes, for both cases where the neutrino/charged lepton track is crossing the rock (denoted as *rock events*) or the water only (denoted as *water events*). Our results can be summarized as follows:

- The impact of the site geography (or matter effects) on observables such as the "rock fraction" of the total event rate or asymmetries in the event direction can be important, particularly at high energies.
- Even for a fixed instrumented volume, these matter effects can be enhanced by a suitable choice of the geometry of the telescope, maximizing the lateral surface of the fiducial volume.
- The continental crust provides an absolute orientation, hence the matter effects may provide a mean for calibrating the pointing capabilities of the detector, even when no point-source identification is possible, like for diffuse cosmic fluxes at UHE.
- We analyzed briefly the dependence of the rock and water events from the neutrino fluxes and the neutrino-nucleon cross section. We found that the ratio of rock to water events may provide an additional way to disentangle the two unknowns, in addition e.g. to the well-known zenith angle dependence of the rates due to the screening effect of the average spherical Earth. Although a detailed analysis would

be needed, we stress that this may be important for constraining neutrino-nucleon cross section at UHE energies, otherwise unaccessible at the Lab.

- While below the PeV scale the aperture for muon tracks is one order of magnitude larger than the aperture for contained events, above $\sim 10^8$ GeV the numbers of muon and tau track events are comparable. We have briefly addressed the problem of whether it is possible to distinguish μ's and τ's in the detector. Apart for the sub-dominant fraction of contained events with specific signatures, we stressed that a realistic prescription at UHE is to sum the bulk of μ and τ events, the natural variables for describing the events being the arrival direction and the energy loss rate in the fiducial volume.

The main conclusion one can draw from our analysis is that the optimization for a telescope aiming at the $E >$PeV region is significantly different from one whose target is the $E \sim$TeV range: in the first case, the search is basically background free and even a relatively poor angular and energy resolution may be acceptable. The crucial goal is to maximize the event rates, and the discrimination among models may be based on "counts" and a very rough directional and energy binning of the events. In this respect, one should maximize the instrumented volume—compatibly with the experimental requirements for a meaningful reconstruction of the event—and also carefully design the geometry to maximize the lateral surface, in order to exploit the matter effects provided by the underwater profile. On the other hand, at TeV energies angular and energy resolutions are crucial to improve the very signal to noise ratio, and may help identifying point-like sources. At the same time, in the TeV range the matter effects we have stressed on in this paper are less relevant, and should not influence significantly the choice of the site.

Acknowledgments

We are pleased to thank G. Barbarino, D. Hooper, G. Longo, and E. Migneco for useful comments and discussions. This work was supported by a Spanish-Italian AI, the Spanish grants FPA2005-01269 and GV/05/017 of Generalitat Valenciana, a MEC-INFN agreement as well as the PRIN04 "Fisica Astroparticellare" of Italian MIUR. SP was supported by a Ramón y Cajal contract of MEC. PS acknowledges the support by the Deutsche Forschungsgemeinschaft under grant SFB 375 and by the European Network of Theoretical Astroparticle Physics ILIAS/N6 under contract number RII3-CT-2004-506222.

References

[1] Berezinsky V S and Zatsepin G T, "Cosmic Rays At Ultrahigh-Energies (Neutrino?)," 1969 *Phys. Lett. B* **28** 423.

[2] Berezinsky V S and Zatsepin G T, "Cosmic Neutrinos Of Superhigh Energy," 1970 *Sov. J. Nucl. Phys.* **11** 111 (1970 *Yad. Fiz.* **11** 200).

[3] Gaisser T K, Halzen F and Stanev T, "Particle Astrophysics With High-Energy Neutrinos," 1995 *Phys. Rep.* **258** 173.
[4] Learned J G and Mannheim K, "High-energy neutrino astrophysics," 2000 *Ann. Rev. Nucl. Part. Sci.* **50** 679.
[5] Spiering C, "High energy neutrino astronomy," 2002 *Prog. Particle Nucl. Phys.* **48** 43.
[6] Halzen F and Hooper D, 2002 "High-energy neutrino astronomy: The cosmic ray connection," *Rept. Prog. Phys.* **65** 1025.
[7] McDonald A B et al., "Astrophysical neutrino telescopes," 2004 *Rev. Sci. Instrum.* **75** 293.
[8] Grieder P K F et al., "DUMAND II: String 1 deployment, initial operation, results and system retrieval," 1995 *Nucl. Phys. Proc. Suppl.* **43** 145.
[9] Balkanov V A et al., "The Lake Baikal Neutrino Telescope NT-200: Status, results, future," 1999 *Nucl. Phys. Proc. Suppl.* **75A** 409.
[10] Andres E et al., "The AMANDA neutrino telescope: Principle of operation and first results," 2000 *Astropart. Phys.* **13** 1.
[11] Ahrens J et al., "Observation of high energy atmospheric neutrinos with the Antarctic Muon and Neutrino Detector Array," 2002 *Phys. Rev. D* **66** 012005.
[12] Belolaptikov I A et al., "The Lake Baikal neutrino experiment: Selected results," 2000 *Phys. Atom. Nucl.* **63** 951.
[13] Ahrens J et al., "Limits on diffuse fluxes of high energy extraterrestrial neutrinos with the AMANDA-B10 detector," 2003 *Phys. Rev. Lett.* **90** 251101.
[14] Halzen F and Hooper D, "AMANDA observations constrain the ultra-high energy neutrino flux," Phys. Rev. Lett. **97**, 099901 (2006)
[15] Ambrosio M et al, 2003 "Search for diffuse neutrino flux from astrophysical sources with MACRO," *Astropart. Phys.* **19** 1.
[16] Aslanides E et al., 1999 "A Deep Sea Telescope for High Energy Neutrinos, Proposal," astro-ph/9907432.
[17] S. Bottai *et al.* [NESTOR Collaboration], 1999 Contribution to 26th ICRC, Salt Lake City, "NESTOR: A status report," Nucl. Phys. Proc. Suppl. **85** (2000) 153.
[18] G. Aggouras *et al.*, "Operation and performance of the NESTOR test detector," Nucl. Instrum. Meth. A **552** (2005) 420.
[19] G. Aggouras *et al.* [NESTOR Collaboration], "A measurement of the cosmic-ray muon flux with a module of the NESTOR neutrino telescope," Astropart. Phys. **23** (2005) 377.
[20] Riccobene G, 2002 Proc. of the Workshop on Methodical Aspects of Underwater/Ice Neutrino Telescopes, 61
[21] Katz U F, "Neutrino telescopy in the Mediterranean sea," 2006 *Prog. Part. Nucl. Phys.* **57** 273.
[22] Katz U F, "KM3NeT: Towards a km**3 Mediterranean neutrino telescope," 2006 [astro-ph/0606068].
[23] J. A. Aguilar *et al.* [ANTARES Collaboration], "First results of the instrumentation line for the deep-sea ANTARES neutrino telescope," Astropart. Phys. **26** (2006) 314 [astro-ph/0606229].
[24] Ahrens J et al., 2000 *The IceCube NSF Proposal.*
[25] Ahrens J et al., 2001 *IceCube Conceptual Design Document.*
[26] Ahrens J et al., "Sensitivity of the IceCube detector to astrophysical sources of high energy muon neutrinos," 2004 *Astropart. Phys.* **20** 507.
[27] R. Gandhi, C. Quigg, M. H. Reno and I. Sarcevic, "Ultrahigh-Energy Neutrino Interactions," Astropart. Phys. **5** (1996) 81 [hep-ph/9512364].
[28] Dutta S I, Reno M H and Sarcevic I, 2000 "Tau-neutrinos underground: Signals of nu/mu —> nu/tau oscillations with extragalactic neutrinos," *Phys. Rev. D* **62** 123001.
[29] González-García M C, Halzen F and Maltoni M, "Physics reach of high-energy and high-statistics Icecube atmospheric neutrino data," 2005 *Phys. Rev. D* **71** 093010.
[30] L. Anchordoqui and F. Halzen, "IceHEP high energy physics at the South Pole," Annals Phys. **321** (2006) 2660 [hep-ph/0510389].

[31] Yoshida S, Ishibashi R and Miyamoto H, "Propagation of extremely-high energy leptons in the earth: Implications to their detection by the IceCube neutrino telescope," 2004 *Phys. Rev. D* **69** 103004.

[32] Beacom J F et al., "Measuring flavor ratios of high-energy astrophysical neutrinos," Phys. Rev. D **68**, 093005 (2003) [Erratum-ibid. D **72**, 019901 (2005)].

[33] Athar H, Parente G and Zas E, "Prospects for observations of high-energy cosmic tau-neutrinos," Phys. Rev. D **62**, 093010 (2000).

[34] Bugaev E, Montaruli T, Shlepin Y and Sokalski I, "Propagation of tau neutrinos and tau leptons through the earth and their detection in underwater / ice neutrino telescopes," Astropart. Phys. **21**, 491 (2004).

[35] Ishihara A (IceCube Collaboration), 2006 *IceCube projects and its EHE physics capability*, Proceedings of CRIS06, Catania (Italy), to appear in *Nucl. Phys. Proc. Suppl.* [astro-ph/0611794].

[36] Beacom J F *et al.*, "Decay of high-energy astrophysical neutrinos," Phys. Rev. Lett. **90**, 181301 (2003)

[37] Beacom J F *et al.*, "Pseudo-Dirac neutrinos, a challenge for neutrino telescopes," Phys. Rev. Lett. **92**, 011101 (2004)

[38] Serpico P D and Kachelrieß M, "Measuring the 13-mixing angle and the CP phase with neutrino telescopes," Phys. Rev. Lett. **94**, 211102 (2005)

[39] Kashti T and Waxman E, "Flavoring astrophysical neutrinos: Flavor ratios depend on energy," Phys. Rev. Lett. **95**, 181101 (2005)

[40] Serpico P D, "Probing the 2-3 leptonic mixing at high-energy neutrino telescopes," Phys. Rev. D **73**, 047301 (2006)

[41] Miele G, Pastor S and Pisanti O, "The aperture for UHE tau neutrinos of the Auger fluorescence detector using a digital elevation map," 2006 *Phys. Lett. B* **634** 137.

[42] Pierre Auger Collaboration, 1996 *The Pierre Auger Project Design Report*, FERMILAB-PUB-96-024.

[43] Abraham J et al. (Pierre Auger Collaboration), "Properties and performance of the prototype instrument for the Pierre Auger Observatory," 2004 *Nucl. Instrum. Meth. A* **523** 50.

[44] Zas E, "Neutrino detection with inclined air showers," 2005 *New J. Phys.* **7** 130.

[45] Capelle K S, Cronin J W, Parente G and Zas E, "On the detection of ultra high energy neutrinos with the Auger Observatory," 1998 *Astropart. Phys.* **8** 321.

[46] Fargion D, Aiello A and Conversano R, 1999 "Horizontal tau air showers from mountains in deep valley: Traces of UHECR neutrino/tau," 1999 Contribution to 26th ICRC, Salt Lake City, *AIP Conf. Proc.* **516** *vol 2 396.*

[47] Becattini F and Bottai S, "Extreme energy nu/tau propagation through the earth," 2001 *Astropart. Phys.* **15** 323.

[48] Fargion D, "Discovering ultra high energy neutrinos by horizontal and upward tau air-showers: First evidences in terrestrial gamma flashes," 2002 *Astrophys. J.* **570** 909.

[49] Letessier-Selvon A, "Establishing the GZK cutoff with ultra high energy tau neutrinos," 2000 *AIP Conf. Proc.* **566** 157.

[50] Bertou X et al., "Tau neutrinos in the Auger observatory: A new window to UHECR sources," 2002 *Astropart. Phys.* **17** 183.

[51] Feng J L, Fisher P, Wilczek F and Yu T M, "Observability of earth-skimming ultra-high energy neutrinos," 2002 *Phys. Rev. Lett.* **88** 161102.

[52] Fargion D, De Sanctis Lucentini P G and De Santis M, "Updated event rate for horizontal and upward tau air showers in EUSO," 2004 *Astrophys. J.* **613** 1285.

[53] Aramo C et al., "Earth-skimming UHE tau neutrinos at the fluorescence detector of Pierre Auger Observatory," 2005 *Astropart. Phys.* **23** 65.

[54] Cao Z, Huang M A, Sokolsky P and Hu Y, "Ultra high energy nu/tau detection using cosmic ray tau neutrino telescope used in fluorescence / Cerenkov light detection," 2005 *J. Phys. G* **31** 571.

[55] Miele G, Perrone L and Pisanti O, "Ultra high energy nu/tau detection at Pierre Auger Observatory," 2005 *Nucl. Phys. Proc. Suppl.* **145** 347.

[56] U.S. Department of Commerce, National Oceanic and Atmospheric Administration, National Geophysical Data Center, 2001 *2-minute Gridded Global Relief Data (ETOPO2)*, `http://www.ngdc.noaa.gov/mgg/fliers/01mgg04.html`

[57] Parameters of the Preliminary Reference Earth Model are given by Adam Dziewonski, Earth Structure, Global, in: *The Encyclopedia of Solid Earth Geophysics*, David E. James, ed. (Van Nostrand Reinhold, New York, 1989) p.331. We use the formula from this work cited in [27].

[58] Halzen F and Saltzberg D, "Tau neutrino appearance with a 1000-Megaparsec baseline," 1998 *Phys. Rev. Lett.* **81** 4305.

[59] L'Abbate A, Montaruli T and Sokalski I, "Effect of neutral current interactions on high energy muon and electron neutrino propagation through the earth," Astropart. Phys. **23**, 57 (2005).

[60] Dutta S I, Huang Y and Reno M H, "Tau neutrino propagation and tau energy loss," 2005 *Phys. Rev. D* **72** 013005.

[61] Waxman E and Bahcall J N, "High energy neutrinos from astrophysical sources: An upper bound," 1999 *Phys. Rev. D* **59** 023002.

[62] Kalashev O E, Kuzmin V A and Semikoz D V, 1999 "Top-down models and extremely high energy cosmic rays," astro-ph/9911035.

[63] Kalashev O E, Kuzmin V A and Semikoz D V, "Ultra high energy cosmic rays propagation in the galaxy and anisotropy," 2001 *Mod. Phys. Lett. A* **16** 2505.

[64] Kalashev O E, Kuzmin V A, Semikoz D V and Sigl G, "Ultra-high energy neutrino fluxes and their constraints," 2002 *Phys. Rev. D* **66** 063004.

[65] Semikoz D V and Sigl G, "Ultra-high energy neutrino fluxes: New constraints and implications," 2004 *JCAP* **0404** 003.

[66] Kachelriess M, Semikoz D V and Tórtola M A, "New hadrons as ultra-high energy cosmic rays," 2003 *Phys. Rev. D* **68** 043005.

[67] Bhattacharjee P and Sigl G, "Origin and propagation of extremely high energy cosmic rays," 2000 *Phys. Rep.* **327** 109.

[68] Anchordoqui L A et al., "Probing Planck scale physics with IceCube," 2005 *Phys. Rev. D* **72** 065019.

[69] Kusenko A and Weiler T J, 2002 "Neutrino cross sections at high energies and the future observations of ultrahigh-energy cosmic rays," *Phys. Rev. Lett.* **88** 161101.

[70] Hooper D, 2002 "Measuring high energy neutrino nucleon cross sections with future neutrino telescopes," *Phys. Rev. D* **65** 097303.

[71] Hussain S , Marfatia D , McKay D W and Seckel D, 2006 "Cross section dependence of event rates at neutrino telescopes," Phys. Rev. Lett. **97**, 161101 (2006).

[72] DeYoung T, Razzaque S and Cowen D F, 2006 "Astrophysical tau neutrino detection in kilometer-scale Cherenkov detectors via muonic tau decay," astro-ph/0608486.

[73] Bottai S and Perrone L, 2001 "Simulation of UHE muons propagation for GEANT3," *Nucl. Instrum. Meth. A* **459** 319.

[74] Barbot C, Drees M , Halzen F and Hooper D, "Neutrinos associated with cosmic rays of top-down origin," 2003 *Phys. Lett. B* **555** 22.

[75] Learned J G and Pakvasa S, "Detecting tau-neutrino oscillations at PeV energies," 1995 *Astropart. Phys.* **3** 267.